THE JOURNAL OF BIOLOGICAL CHEMISTRY VOL. 284, NO. 46, pp. 31817–31826, November 13, 2009

A Conserved Membrane Attachment Site in α-SNAP Facilitates *N*-Ethylmaleimide-sensitive Factor (NSF)-driven SNARE Complex Disassembly*[S]

Received for publication, July 17, 2009, and in revised form, September 15, 2009 Published, JBC Papers in Press, September 17, 2009, DOI 10.1074/jbc.M109.045286

Ulrike Winter, Xiong Chen[1], and Dirk Fasshauer[2]

From the Research Group Structural Biochemistry, Department of Neurobiology, Max Planck Institute for Biophysical Chemistry, Am Fassberg 11, 37077 Göttingen, Germany

The ATPase NSF (*N*-ethylmaleimide-sensitive factor) and its SNAP (soluble *N*-ethylmaleimide-sensitive factor attachment protein) cofactor constitute the ubiquitous enzymatic machinery responsible for recycling of the SNARE (SNAP receptor) membrane fusion machinery. The enzyme uses the energy of ATP hydrolysis to dissociate the constituents of the SNARE complex, which is formed during the fusion of a transport vesicle with the acceptor membrane. However, it is still unclear how NSF and the SNAP adaptor work together to take the tight SNARE bundle apart. SNAPs have been reported to attach to membranes independently from SNARE complex binding. We have investigated how efficient the disassembly of soluble and membrane-bound substrates are, comparing the two. We found that SNAPs support disassembly of membrane-bound SNARE complexes much more efficiently. Moreover, we identified a putative, conserved membrane attachment site in an extended loop within the N-terminal domain of α-SNAP. Mutation of two highly conserved, exposed phenylalanine residues on the extended loop prevent SNAPs from facilitating disassembly of membrane-bound SNARE complexes. This implies that the disassembly machinery is adapted to attack membrane-bound SNARE complexes, probably in their relaxed cis-configuration.

All intracellular vesicle transport processes, ranging from secretion in yeast to neurotransmitter release in the brain, depend on the ability of membranes to fuse with each other. Intracellular fusion is mediated by the soluble *N*-ethylmaleimide-sensitive factor attachment protein receptor (SNARE)[3] proteins on opposing membranes, which assemble in trans-configuration into four-helix bundle complexes, bringing the membranes into close proximity (for an overview see Refs. 1–4). After fusion, all SNAREs constituting one complex are anchored in a relaxed cis-configuration to one membrane and are no longer free to act in further cycles of fusion. These cis-SNARE complexes were found to be extremely stable, with basically no spontaneous dissociation detectable (5–7). Thus, in order to recycle the fusion machinery, these complexes need to be dissociated actively. To achieve this, the cell exploits the AAA ATPase NSF (*N*-ethylmaleimide-sensitive factor), which couples ATP hydrolysis to the thermodynamically unfavorable dissociation of the SNARE bundle.

Despite its fundamental role in the cell, surprisingly little progress has been made in deciphering the molecular details of NSF action since its discovery about 30 years ago (8). It is thought that for disassembly, ring-shaped NSF hexamers (9–11) attack SNARE bundles standing upright in the membrane at their N-terminal side (12). As SNARE complexes do not display a direct binding site for NSF, SNAPs (soluble NSF attachment proteins) (13), very probably in three copies (14), have to serve as adaptors between the SNARE complex and the enzyme. The entire disassembly complex is referred to as the 20S complex (15, 16). Although high-resolution structures of several components and domains are available, neither the structure of the complete NSF molecule nor of the 20S complex is known in sufficient detail. Hence, the molecular details of the arrangement of the molecules in the 20S particle are elusive (17–19).

A milestone on the way toward rebuilding SNARE disassembly from scratch has recently been achieved (20, 21). A new *in vitro* assay with high time resolution has been established. This assay uses recombinant SNAREs fused to GFP (green fluorescent protein) analogs as substrates and monitors the disassembly reaction spectroscopically. Interestingly, even though the amounts of NSF the authors reported for efficient disassembly were reasonably low for enzymatic reactions, α-SNAP (*i.e.* one of the three SNAP isoforms in vertebrates) was required in surprisingly high concentrations. Because this assay does not allow for direct quantification of α-SNAP/SNARE binding, the α-SNAP/SNARE complex affinity was determined using GST (glutathione *S*-transferase)-coupled SNARE complexes. This led to an EC_{50} of 5 μM at a complex concentration of only 100 nM, suggesting that α-SNAP has a very low affinity for the SNARE complex (20). Comparably low α-SNAP affinities have also been observed by other groups pursuing *in vitro* matrix-based studies of the affinity between α-SNAP and SNARE com-

* This work was supported by the SFB523 of the Deutsche Forschungsgemeinschaft (to U. W.).

[S] The on-line version of this article (available at http://www.jbc.org) contains supplemental Figs. S1–S4.

[1] Present address: Institut de Biologie Physico-Chimique, CNRS UPR 1929, 13, rue P. et M. Curie, F-75005 Paris, France.

[2] To whom correspondence should be addressed. Tel.: 49-551-201-1637; E-mail: dfassha@gwdg.de.

[3] The abbreviations used are: SNARE, SNAP receptor; NSF, *N*-ethylmaleimide-sensitive factor; SNAP, soluble NSF attachment protein; SNAP-25, synaptosomal-associated protein of 25 kDa; VAMP, vesicle-associated membrane protein; Cpx1, complexin 1; Syx, syntaxin; Syb, synaptobrevin; OG, Oregon Green; TR, Texas Red; AAA proteins, ATPases associated with various cellular activities; DDM, n-dodecyl-β-D-maltoside; GST, glutathione *S*-transferase; GFP, green fluorescent protein; FRET, Förster Resonance Energy Transfer; CHAPS, 3-[(3-cholamidopropyl)dimethylammonio]-1-propanesulfonic acid; aa, amino acids.

plexes (22, 23). Besides the fact that this high demand for α-SNAP for disassembly probably has no physiological basis, it also is at odds with findings from other experiments (24, 25), in which optimal function was reconstituted using much lower amounts of α-SNAP (~0.6 μM). For example, in a study we published recently, we found that disassembly reached optimal speed at an α-SNAP concentration of ~100 nM when monitoring disassembly in a more physiological system, the so-called membrane sheets (26).

So why are there such marked differences between different systems and studies? One possible explanation for variances in α-SNAP efficiency may be experimental constraints, *e.g.* a loss of α-SNAP functionality under certain conditions. Alternatively, an additional and as yet unknown player might be important for optimal α-SNAP function that is only present in physiological systems. To investigate whether a hitherto unrecognized factor contributes to optimal SNAP reactivity, we therefore chose to establish a reductionist approach based on fluorescence spectroscopy, which directly monitors SNAP/SNARE and SNARE/SNARE interactions in a time-resolved manner.

EXPERIMENTAL PROCEDURES

Protein Constructs—Besides the expression constructs for the yeast disassembly proteins Sec17 and Sec18 in pQE19-vectors (27) (kindly provided by C. Ungermann, Osnabrück, Germany), and β-SNAP in pGEX-2T, all other recombinant proteins were in a pET28a or pET15b vector (Novagen, Schwalbach, Germany), which encode for an N-terminal His_6 tag that can be cleaved by thrombin. The following constructs derived from rat cDNAs have been described earlier (28–31): cysteine-free SNAP25a (aa 1–206), soluble synaptobrevin 2 (aa 1–96, Syb), synaptobrevin 2 full-length (aa 1–116, SybTMD), the soluble SNARE domain of syntaxin 1a (aa 180–262, SyxH3), full-length syntaxin 1a (aa 1–288), and complexin 1 (Cpx 1). We also used the single cysteine variants of SNAP-25, $SNAP25^{C130}$ (32), and synaptobrevin (aa 1–96, Syb^{C28} and aa 1–116, $SybTMD^{C28}$) that have been described previously (33). The recombinant proteins encoding for bovine α-SNAP (aa 1–295) and β-SNAP (aa 1–298) were recloned into the pET28a vector as described earlier (34), as were recombinant proteins encoding for NSF in Chinese hamster (kindly provided by J. E. Rothman, New Haven, CT). All these recombinant proteins were originally in pQE9 vectors. In addition, we used the single point mutation Leu-294 of α-SNAP, $\alpha\text{-SNAP}^{L294A}$ (35), which was generated earlier (34). The following constructs were newly generated for this study: a deletion variant of α-SNAP in which the first 32 residues were removed ($\alpha\text{-SNAP}^{del}$ (aa 33–295)) and an α-SNAP mutant in which the two phenylalanines in positions 27 and 28 were mutated to serines ($\alpha\text{-SNAP}^{F27S,F28S}$). In addition, the following yeast SNARE protein constructs were generated: the SNAP-25-like domain of Sec9 (aa 403–651), a single cysteine variant of Sec9 (aa 403–651, Cys-587), a full-length Snc2 (aa 1–115, Snc2TMD), the soluble region of Snc2 (aa 1–93), the single cysteine variant of Snc2 (aa 1–93, Cys24), and SNARE motifs of Sso1 with (aa 179–290) and the other without the transmembrane domain (aa 179–264).

Purification of Recombinant Proteins—All proteins were expressed in *Escherichia coli* strain BL21 (DE3) and purified by Ni^{2+}-nitrilotriacetic acid (NTA) affinity, except Sec17 and Sec18, followed by thrombin cleavage of either the His_6 tags during overnight dialysis. In the case of β-SNAP, GST affinity chromatography was used for purification, and thrombin cleavage was performed on the GST tag on the column. To achieve a high grade of purity, all proteins were subsequently subjected to a second chromatographic step on an Äkta system (GE Healthcare). In the case of the SNAPs and SNAREs this was achieved by ion exchange as previously described (28, 29, 33). After elution from the Ni^{2+}-NTA resin, NSF and Sec18 were dialyzed against 50 mM HEPES (pH 7.4), 175 mM NaCl, 1 mM EDTA, 2 mM dithiothreitol, 0.5 mM ATP, and 10% glycerol. They were then purified by size exclusion chromatography on a Superdex-200 column. Purification of proteins containing a transmembrane domain was done in the presence of 15 mM CHAPS as described earlier (36). SNARE complexes were assembled overnight before purification by ion exchange chromatography.

Liposome Preparation—Liposome preparation was done as previously described (36). The lipids (Avanti Polar Lipids) phosphatidylcholine, phosphatidylethanolamine, phosphatidylserine, phosphatidylinositol, and cholesterol were mixed in molar ratio of 5:2:1:1:1 in an argon atmosphere. This lipid composition is comparable to the composition reported for synaptic vesicles (37, 38). After drying, the lipid mix was resuspended in HB100 (50 mM HEPES, pH 7.4, 100 mM KCl) containing 5% (w/v) sodium cholate at a total lipid concentration of 13.5 mM. Transmembrane SNARE complexes in 5% CHAPS were added to the lipid mix at a lipid-to-protein molar ratio of 200:1 after overnight incubation. The protein-lipid mix was incubated at 4 °C for 30 min followed by size exclusion chromatography on a SMART system using a PC 3.2/10 Fast Desalting column (GE Healthcare) equilibrated in HB100. In addition, protein-free liposomes containing 1.5% NBD (4-nitrobenzo-2-oxa-1,3-diazole) and 1.5% rhodamine coupled to phosphatidylethanolamine were prepared. Solubilization of these liposomes using the detergent n-dodecyl-β-D-maltoside (DDM) was monitored by Förster Resonance Energy Transfer (FRET) at $\lambda_{ex} = 460$ nm and $\lambda_{em} = 530$ nm and 585 nm.

Disassembly Reaction—For disassembly, a buffer containing KGlu/KAc at concentrations of 120 mM and 20 mM respectively, as well as 2 mM ATP, 5 mM $MgCl_2$ and 50 mM HEPES (pH 7.4) was used. Covalent attachment of the sulfhydryl-reactive fluorophores Oregon Green 488 iodoacetamide (OG) or Texas Red C5 bromoacetamide (TR) or Alexa594 C_5 maleimide (Invitrogen) to the respective SNARE proteins was performed according to the manufacturer's instructions. Typically, SNARE complexes used for fluorescence anisotropy measurements were purified by ion-exchange chromatography and labeled afterward at the single cysteine residue. SNARE complexes used for FRET measurements, if not indicated otherwise, were generated by incubation of stoichiometric amounts of the SNAREs. Complex formation was then monitored spectroscopically. The disassembly enzymes were added at the concentrations indicated.

Fluorescence Measurements—Measurements were carried out in a Fluorolog 3 spectrometer in T-configuration equipped

for polarization (Model FL322, Horiba Jobin Yvon) or a Fluoromax 2 Instrument (Horiba Jobin Yvon). All measurements were carried out at 37 °C in quartz cuvettes (Hellma) in a disassembly buffer. FRET experiments were recorded by excitation at 488 nm, monitoring donor (OG) fluorescence emission at 520 nm and acceptor (TR or Alexa594) fluorescence emission at 610 nm. Typically, the slit widths were set to 1 nm for the excitation wavelength, 2 nm for the donor and 4 nm for the acceptor, and the integration time was set to 1 s. Fluorescence anisotropy was measured using Texas Red-labeled proteins and a slit width of 3 nm for the excitation wavelength (520 nm) and 5 nm for the emission wavelength (610 nm), respectively. The *G* factor was calculated according to $G = I_{HV}/I_{HH}$, where I is the fluorescence intensity, the first subscript letter indicates the direction of the exciting light, and the second subscript letter the direction of emitted light. The intensity of the vertically (V) and horizontally (H) polarized emission light after excitation by vertically polarized light was measured. The anisotropy (r) was determined according to $r = (I_{VV} - G\,I_{VH})/(I_{VV} + 2\,G\,I_{VH})$.

RESULTS

FRET and Fluorescence Anisotropy Can Monitor SNARE Complex Disassembly in Vitro—To monitor the assembly of the neuronal SNARE complex in real time, we had previously developed fluorescence assays (30). We took advantage of these assays to investigate the reverse reaction, the breaking up of the four-helix bundle SNARE complex by NSF and its SNAP cofactor.

For FRET measurements, we generally mixed the three SNARE proteins, two of which were specifically labeled, in stoichiometric amounts. SNARE complex formation was readily identified by a marked increase in donor fluorescence (30). Upon addition of NSF, α-SNAP and free Mg^{2+}, a reduction of energy transfer occurred. Fig. 1 shows a typical FRET measurement, in which a FRET pair in the N-terminal region of the complex was used, *i.e.* synaptobrevin labeled at position 28 with Texas Red (Syb^{C28TR}) and SNAP-25 labeled at position 130 with Oregon Green ($SNAP25^{C130OG}$).

For fluorescence anisotropy measurements, we routinely used a SNARE complex labeled with Texas Red at Syb^{C28}. The readout here depends on the flexibility of the dye, which changes upon interaction of the labeled protein with other proteins. Indeed, addition of α-SNAP alone caused a significant increase of fluorescence anisotropy before disassembly was even initiated. The same increase in anisotropy was observed when $\alpha\text{-SNAP}^{wt}$ was substituted by the mutant $\alpha\text{-SNAP}^{L294A}$, which was not able to support disassembly (35). Interestingly, when enzymatic amounts of NSF were subsequently added, no further signal change was observed. However, when much higher concentrations of NSF were added, an additional increase in fluorescence anisotropy was observed (data not shown), which probably signifies the formation of the 20S complex. When we finally triggered disassembly with $MgCl_2$, the reaction proceeded efficiently as can be seen by a gradual decrease of fluorescence anisotropy (Fig. 1*d*). The rate of disassembly is comparable to the one observed in the FRET measurements, underlining the validity of both methods. In the following, the buffering conditions were optimized, eventually leading to a standard composition for disassembly buffer, which includes KGlu/KAc at concentrations of 120 and 20 mM, respectively, as well as 2 mM ATP, 5 mM $MgCl_2$, and 50 mM HEPES, pH7.4.

α-SNAP Efficiency Is Low in Solution—To determine the optimal concentrations of NSF, ATP, and α-SNAP under the conditions used in the fluorescence assays, we monitored disassembly kinetics, varying the concentration of one of these factors at a time. As shown in supplemental Fig. S1, the ATP and NSF requirements were in line with earlier studies (39).

Also in line with earlier findings (20, 21), micromolar amounts of α-SNAP were needed for efficient disassembly. As outlined above, an advantage of the fluorescence anisotropy approach is that it can also serve as a monitor of α-SNAP binding, although the small change in anisotropy renders it difficult to quantify the exact amount of bound molecules. Nevertheless an optimal increase in fluorescence anisotropy was observed only at higher α-SNAP concentrations (Fig. 2*a*), suggesting that α-SNAP binds with only moderate affinity to the soluble SNARE complex. Keeping in mind that the stoichiometry of 20S complexes has been reported to be 6:3:1 (NSF:α-SNAP:SNARE complex) and that NSF does not interact with α-SNAP in solution (14), the need for such high α-SNAP amounts to saturate SNARE complex binding is not likely to be physiological.

In principle, the low α-SNAP efficiency could be inherent to the recombinant α-SNAP, possibly due to invisible degradation or a lack of putative posttranslational modifications. Nevertheless, we have recently shown that our recombinant α-SNAP disassembles SNARE complexes on sheets of PC12-cell membranes efficiently when applied in a concentration of less than 100 nM (26). The apparently high α-SNAP affinity in the sheet experiments strongly suggested that a factor that is missing in the experiments using the soluble SNARE complex but present on membrane sheets is responsible for the different α-SNAP efficiency.

SNARE Complex Incorporation into Liposomes via Their Transmembrane Domains Potentiates α-SNAP Efficiency—Considering that the disassembly reaction in the cell is most likely to occur only after vesicle fusion is complete and all three SNAREs are located on one membrane, it was tempting to speculate that the membrane is of some importance during the disassembly reaction. To test this hypothesis, measurements were carried out using SNARE complexes incorporated into liposomes. Indeed, α-SNAP turned out to be more potent in disassembling SNARE complexes on liposomes than in solution. This is illustrated in Fig. 3*a*, where decreasing amounts of α-SNAP were used. As little as 30 nM α-SNAP promoted disassembly, 45 nM sufficed to disassemble all complexes and 120 nM saturated the assay, which is very similar to the requirements observed in the sheet assay (26). A direct comparison of α-SNAP efficiency on liposomes and in solution (Fig. 3*b*) furthermore illustrates that the improvement on liposomes is quite substantial: In solution, roughly 20 times more α-SNAP is required to reach comparable kinetics as on liposomes. The α-SNAP dependence on liposomes was identical regardless of which SNARE transmembrane domain (synaptobrevin or syntaxin) was used for complex incorporation. This renders it

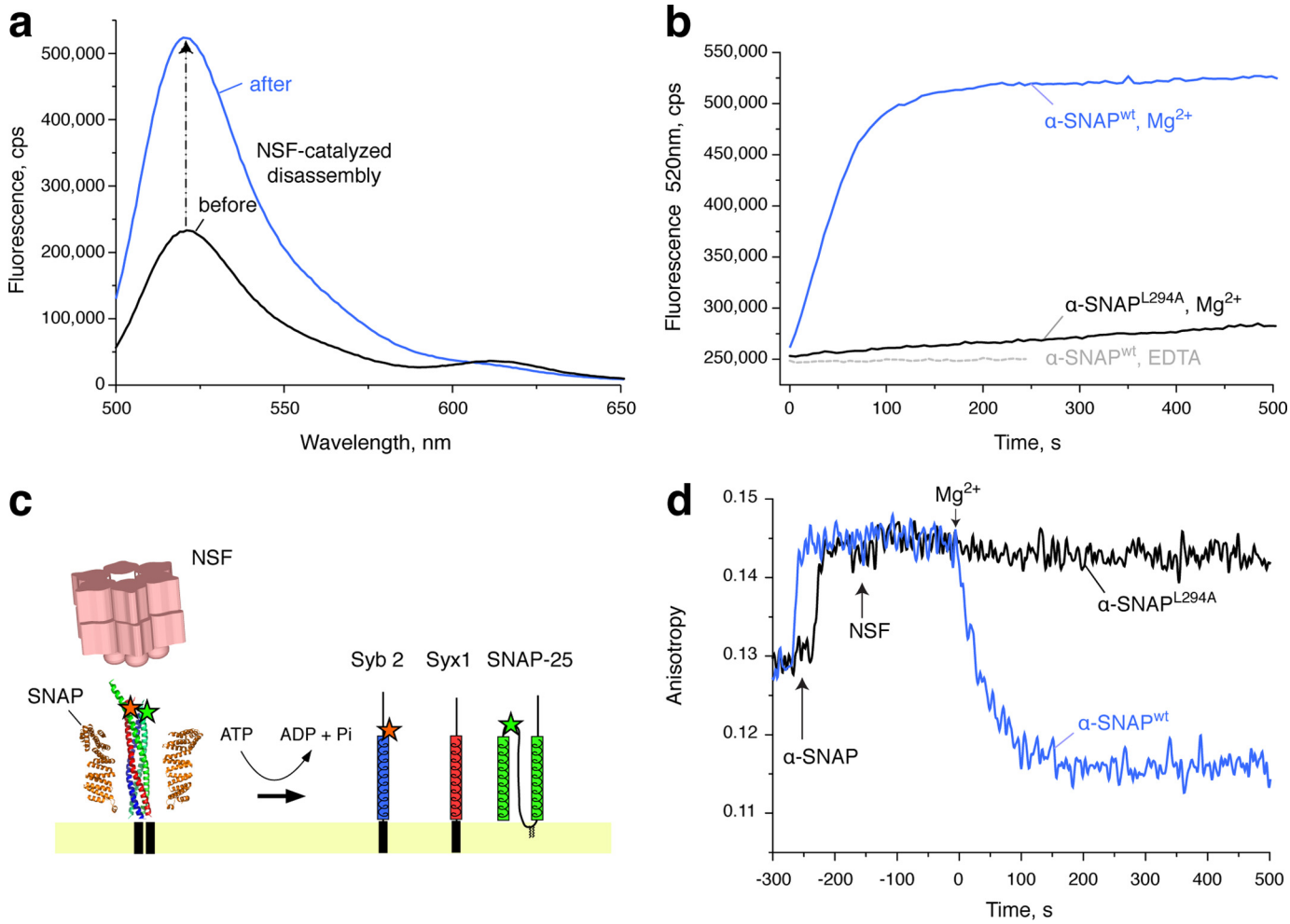

FIGURE 1. ***In vitro* SNARE complex disassembly monitored by fluorescence spectroscopy.** A SNARE complex was pre-assembled composed of synaptobrevin labeled at position 28 with Oregon Green, SNAP-25 labeled at position 130 with Texas Red, and the SNARE motif of syntaxin (Syb^{C28TR}: SNAP25^{C130TR}: SyxH3). 1 μM of unlabeled synaptobrevin (residues 1–81; to prevent reformation of FRET active SNARE complexes), 1 μM α-SNAP (wild-type or L294A mutant), and 1 mM ATP were added to about 100 nM of the double-labeled SNARE complex. The reaction was then started through the addition of ≈0.5 μM NSF. *a*, fluorescence spectrum of the SNARE complex before and after disassembly obtained upon excitation at 488 nm. *b*, change in the donor fluorescence at 520 nm upon disassembly. Disassembly readily occurred in the presence of wild-type α-SNAP (α-SNAP^{wt}) and free Mg^{2+}, whereas chelating Mg^{2+} with EDTA or the presence of the none-functional α-SNAP mutant L294A (35) (α-SNAP^{L294A}) blocked the reaction. *c*, schematic depiction of the disassembly reaction monitored by fluorescence. The label positions in synaptobrevin 2 and SNAP-25 are shown as *asterisks*. *d*, disassembly monitored by fluorescence anisotropy. In this stage, 150 nM of purified SNARE complex containing synaptobrevin labeled at position 28 with Texas Red (Syb^{C28TR}:SNAP25:SyxH3) was disassembled in the presence of 2 mM ATP and 1.2 μM α-SNAP. Note that the addition of α-SNAP^{wt} or α-SNAP^{L294A} led to an initial increase of fluorescence anisotropy in the absence of NSF, demonstrating that this read-out is also able to detect binding of α-SNAP. No significant change in fluorescence anisotropy was detected upon addition of 10 nM NSF before the reaction was triggered by addition of 5 mM Mg^{2+} (*arrow*).

unlikely that the presence of the membrane anchors caused the increased α-SNAP efficiency.

At this point, we did not know whether the actual anchorage of the complex to the membrane is a prerequisite for the markedly improved α-SNAP performance or whether the mere presence of the hydrophobic transmembrane domains or lipids leads to an increased α-SNAP efficiency. To resolve this question, we treated liposome-incorporated SNARE complexes with detergent prior to disassembly to dissolve the liposomes, carefully staying below concentrations that would be harmful for the disassembly machinery. Indeed, stepwise dissolution of liposomes by application of detergent correlated with a stepwise reduction of the fraction of SNARE complexes that were quickly disassembled. This indicates that the SNARE complexes indeed need to be anchored to the membrane to serve as high affinity targets of α-SNAP (see supplemental Fig. S2).

Design of α-SNAP Mutants Lacking the Putative Lipid-interacting Domain—α-SNAP is an amphiphilic protein that has been reported to bind even to plastic surfaces (40, 41) Furthermore, α-SNAP was shown to bind lipids independently of SNAREs (42). Alongside these observations, the data collected so far made it tempting to speculate that a direct interaction between α-SNAP and the membrane lipids is responsible for the increased α-SNAP efficacy on liposomes. If this were true, the lipid binding property might possibly be mapped to a certain region of α-SNAP. No crystal structure has been solved for α-SNAP so far, but the structures of the γ-SNAP isoform (43) and of the yeast homolog Sec17 are known (44). Based on interaction studies using various point-mutated α-SNAPs, a model of α-SNAP bound to the SNARE complex has been proposed by Marz *et al.* (20). According to this model, mostly basic residues on the conserved ridge of α-SNAP form a diagonal band across

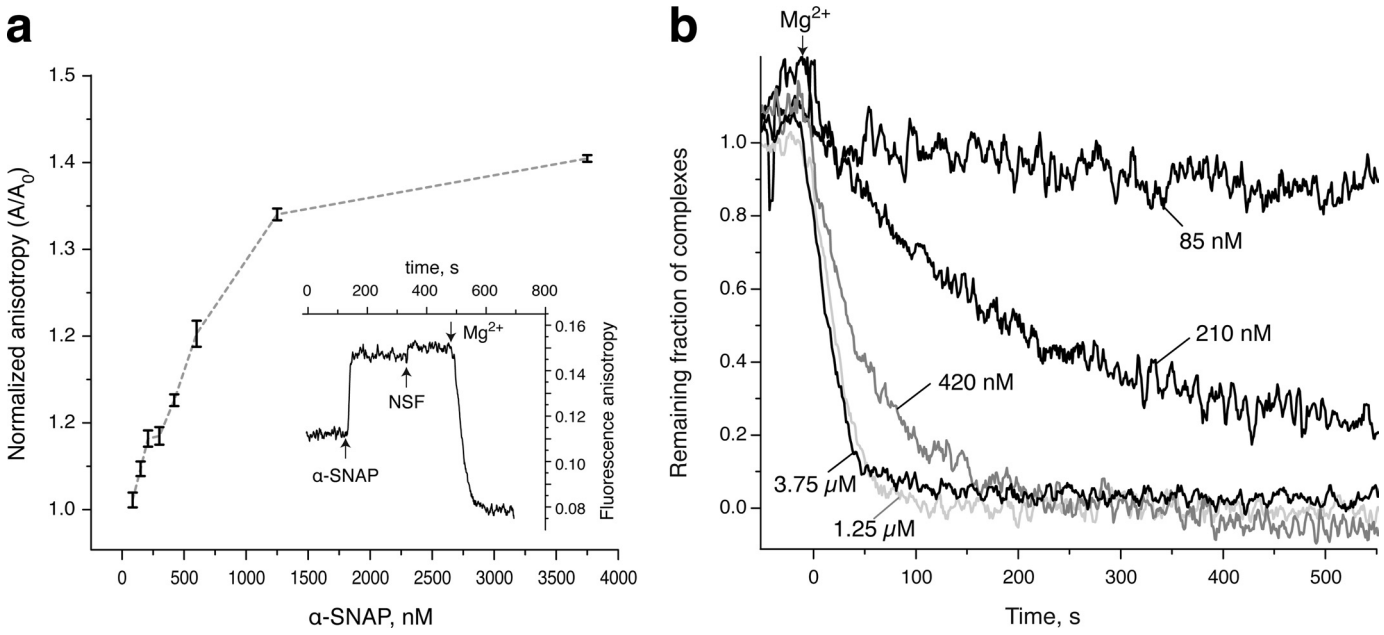

FIGURE 2. **Micromolar amounts of α-SNAP are required for efficient disassembly of the soluble SNARE complex.** *a*, binding of α-SNAP to the purified labeled SNARE complex (Syb^{C28TR}:SNAP25:SyxH3, 75 nM) leads to increase of fluorescence anisotropy in the absence of NSF. The signal changes upon binding of increasing amounts of α-SNAP are shown as multiples of the anisotropy prior to addition of α-SNAP. Mean values of anisotropy change are plotted against the α-SNAP concentration. Adding NSF in the absence of Mg^{2+} leads to a further increase in anisotropy. The disassembly reaction was then started by the addition of 5 mM $MgCl_2$. A typical sequence of fluorescence changes is shown in the *inset* (1.5 μM α-SNAP was added). *b*, subsequently, the disassembly reaction was followed by a decrease in fluorescence anisotropy. To compensate for the differences in the starting value of fluorescence anisotropy resulting from the different amounts of bound α-SNAP, the reactions were normalized. For disassembly, 10 nM NSF and 2 mM ATP were added, and the reaction was started by addition of 5 mM $MgCl_2$. Note that an optimal binding and reaction rate was reached only at about 1.25 μM α-SNAP.

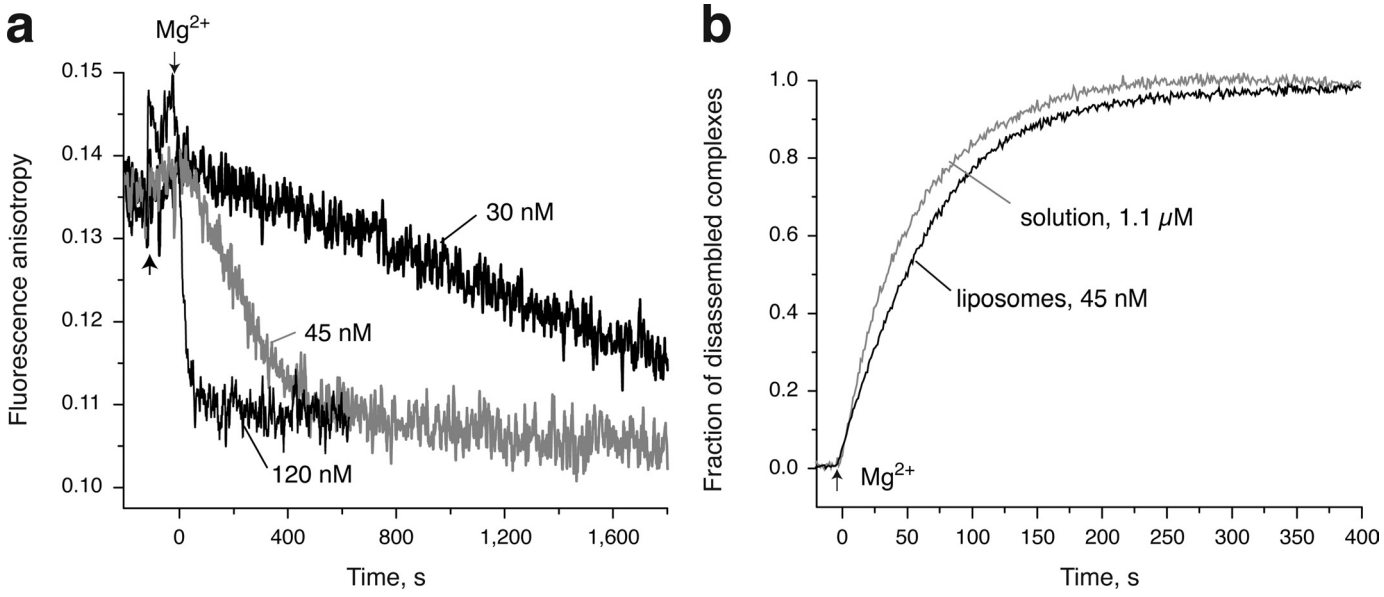

FIGURE 3. **Incorporating the SNARE complexes into liposomes renders α-SNAP more efficient.** *a*, disassembly kinetics of the liposomal SNARE complex (SybTMR^{C28TR}:SNAP25:SyxH3, ~35 nM) using different amounts of α-SNAP. The reaction in the presence of 5 nM NSF and 2 mM ATP was started by adding 5 mM $MgCl_2$. Note that 120 nM α-SNAP sufficed to promote fast disassembly of membrane-inserted SNARE complexes. *b*, to disassemble soluble SNARE complexes (Syb^{C28TR}:SNAP25:SyxH3) at approximately similar speed as observed for liposomal SNARE complexes (SybTMR^{C28TR}:SNAP25:SyxH3), more than 20 times more α-SNAP had to be added.

that interacts with a complementary stretch on the SNARE complex bundle. Within the 32 very N-terminal residues of the α-SNAP homology model, an arm-like structure points away from the complex. This arm consists of a loop of mostly hydrophobic amino acids (residues 27–32) that are highly conserved in different SNAPs, as can be gleaned from a sequence alignment shown in Fig. 4*a*. If this region were the interaction site of α-SNAP with the membrane as suggested by the depiction in Fig. 4*b*, its deletion should interfere with membrane binding and hence the higher α-SNAP efficiency on membranes. We chose to design two mutants: One large-scale deletion (deleting residues 1–32) mutant designated α-SNAP^{del}, and a subtler one, where the mutations were confined to only the loop region. In detail, we changed two

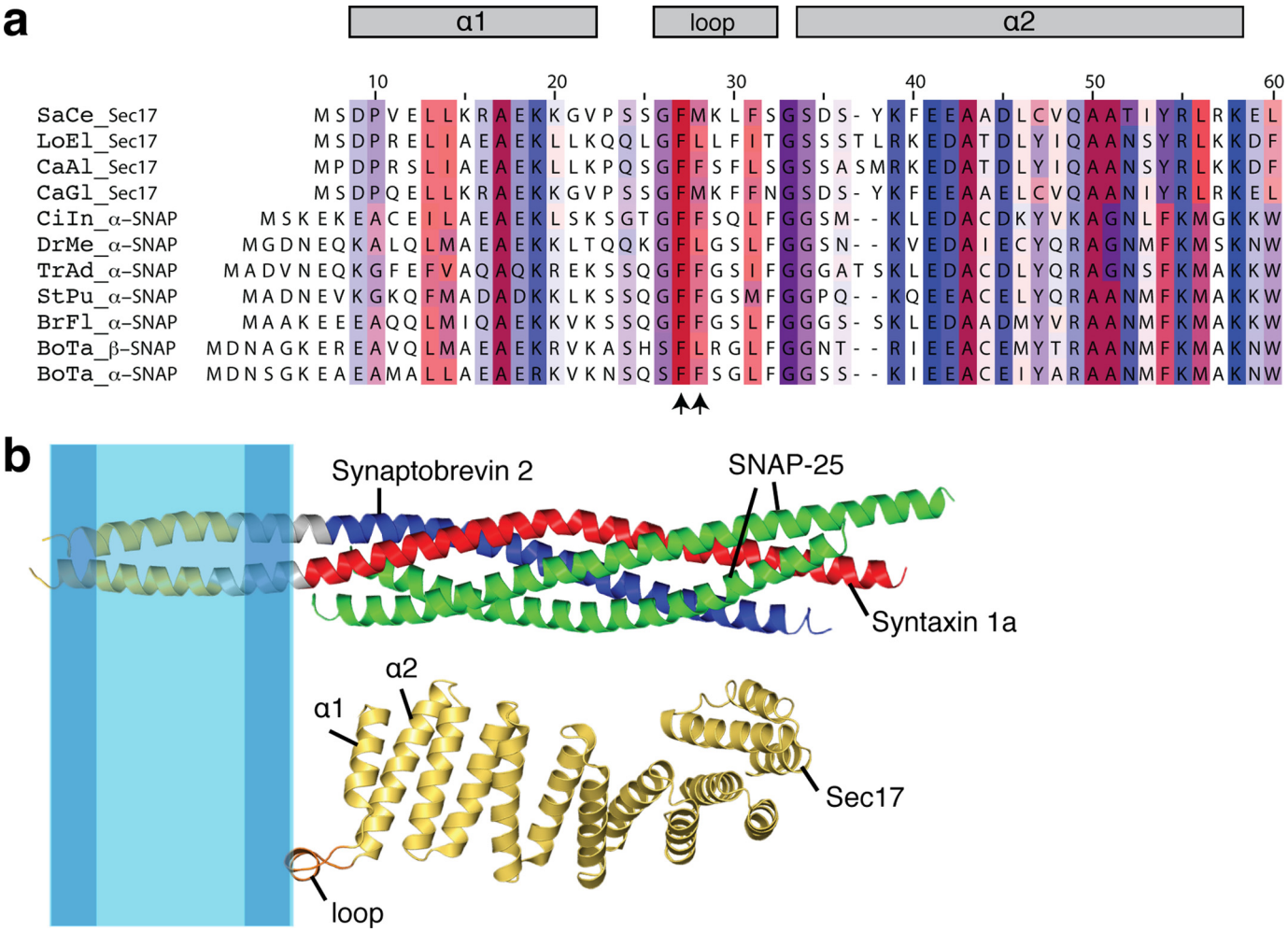

FIGURE 4. **A hydrophobic loop in the N-terminal region of SNAP might serve as membrane attachment site.** *a*, structure-based sequence alignment of the N-terminal portion of SNAP proteins from different organisms indicates that the hydrophobic loop between the first two helices is conserved. At the top, *boxes* indicate the first two helices and the connecting loop from the Sec17 crystal structure. The yeast Sec17 (SaCe_Sec17, *Saccharomyces cerevisiae*, gi 6319421) was aligned with several fungal and animal SNAP homologs: LoLe_Sec17, *Lodderomyces elongisporus*, gi 149246407; CaAl_Sec17, *Candida albicans*, gi 68475136; CaGl_Sec17, *Candida glabrata*, gi 50287489; CiIn_α-SNAP, *Ciona intestinalis*, gi 198424864; DrMe_α-SNAP, *Drosophila melanogaster*, gi 17737681; TrAd_α-SNAP, *Trichoplax adhaerens*, gi 196014845; StPu_α-SNAP, *Strongylocentrotus purpuratus*, gi 72082731; BrFl_α-SNAP, *Branchiostoma floridae*, gi 219425561; and BoTa_β-SNAP, *Bos taurus*, gi 423236; BoTa_α-SNAP, *Bos taurus*, gi 423230. *Arrowheads* indicate the highly conserved aromatic residues that were mutated to serines. *b*, schematic drawing of the crystal structures of Sec17 from Baker's yeast (PDB code 1QQE, *S. cerevisiae*) (56) and of the membrane-embedded neuronal SNARE complex including its transmembrane regions (Ref. 57, PDB codes 3HD7 and 3HD9). This illustration indicates that the loop between the first two helices of Sec17 might touch the membrane when the protein is bound to the SNARE bundle. Note that the illustration is largely based on the model of the α-SNAP: SNARE complex interaction given in Marz *et al.* (20).

conserved phenylalanines (residues 27 and 28) for the polar amino acid serine (α-SNAP^{F27S,F28S}).

Both Mutated α-SNAPs Have Lost the Lipid-mediated Efficiency Boost—We found that both mutants were able to disassemble soluble SNARE complexes. α-SNAP^{F27S,F28S} turned out to promote disassembly of soluble SNARE complexes as efficiently as wild-type α-SNAP (Fig. 5*a*), whereas α-SNAP^{del} was somewhat less efficient. The latter was not surprising, because a deletion of residues 1–28 had been reported to hamper SNAP efficiency before (25). We therefore chose to concentrate on the less severe α-SNAP mutant, α-SNAP^{F27S,F28S}. We directly compared its disassembly kinetics in solution and on liposomes of α-SNAP^{F27S,F28S} and of α-SNAP^{wt}, using the fluorescence anisotropy set-up. Knowing that α-SNAP^{wt} efficiency increases 20-fold on liposomes, we employed ~20-fold less of the respective α-SNAP (60 nM) for the experiments on liposomes, leaving everything else as in solution. Remarkably, whereas 60 nM α-SNAP^{wt} efficiently promoted disassembly of membrane-inserted SNARE complexes, the same amount of α-SNAP^{F27S,F28S} did not support disassembly on liposomes at all (Fig. 5*b*). Increasing the concentration of α-SNAP^{F27S,F28S} led to a gradual increase of disassembly speed on liposomes. When we also tested the α-SNAP^{del} mutant, notwithstanding its reduced overall α-SNAP efficiency, we found that the membrane-mediated α-SNAP-potentiation was also abolished (supplemental Fig. S3). Together, these findings suggest that the arm-like structure at the N-terminal tip of α-SNAP might serve as a hitherto unknown membrane attachment site.

The Membrane Boost Is Conserved for Other SNAP Proteins—We next asked whether the membrane boost is conserved for other homologs of the disassembly machinery. To answer this question, we focused on the mammalian brain-specific SNAP isoform β-SNAP and the SNAP homolog of yeast, Sec17 (13, 45).

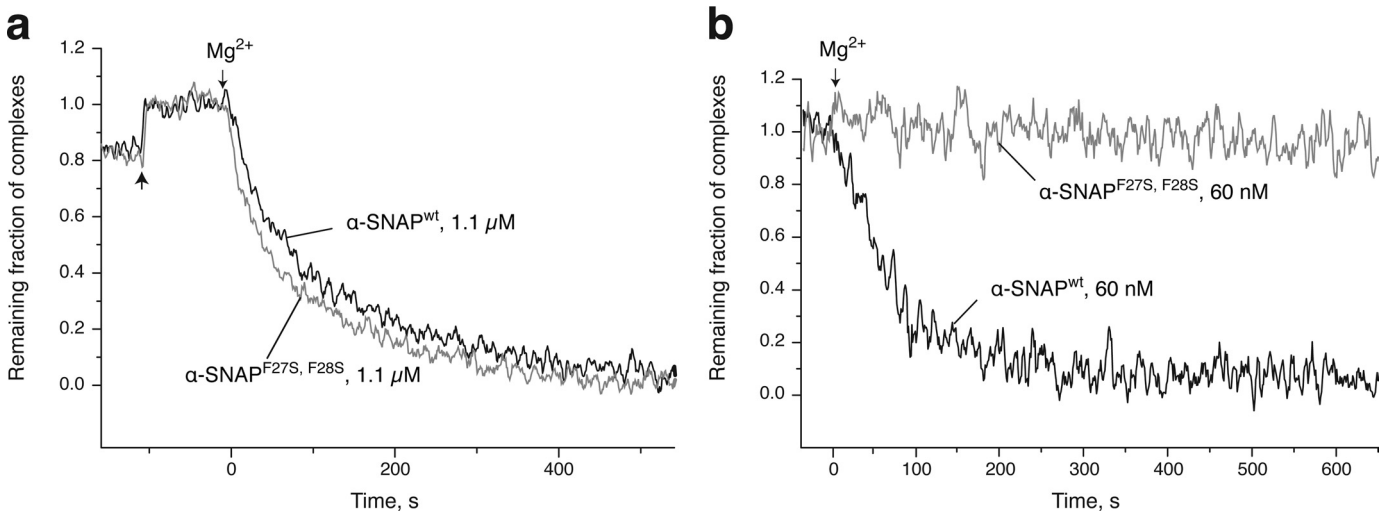

FIGURE 5. **On liposomes, the mutant α-SNAP^{F27S,F28S} does not show the increased efficiency seen for wild-type α-SNAP.** *a*, α-SNAP^{wt} and α-SNAP^{F27S,F28S} support disassembly of soluble SNARE complexes with comparable efficiency. Disassembly of ~80 nM labeled SNARE complex (Syb^{C28TR}:SNAP25:SyxH3) was monitored by fluorescence anisotropy. Both α-SNAP variants were employed at 1.1 μM in the presence of 3 nM NSF. *b*, α-SNAP^{wt} supported disassembly of liposomal SNARE complexes (SybTMR^{C28TR}:SNAP25:SyxH3) at 60 nM concentration, whereas no disassembly was observed when 60 nM α-SNAP^{F27S,F28S} were employed.

Because of the high sequence similarity of β-SNAP and α-SNAP, we were not surprised to find that β-SNAP behaved very similar to α-SNAP with respect to promoting disassembly. Like α-SNAP, β-SNAP was also more efficient in disassembling SNARE complexes in membranes (supplemental Fig. S4).

To investigate the activity of the yeast SNAP Sec17, we first established that the yeast enzymes could substitute for their mammalian counterparts. Strikingly, both the yeast and the mammalian disassembly machinery were able to disassemble the neuronal SNARE complex as well as the yeast complex (data not shown), although the neuronal disassembly machinery was clearly more efficient, possibly because of the higher purity and stability of these proteins. We then compared Sec17 function on liposomes and in solution (Fig. 6). Here, the Sec17-concentration capable of mediating disassembly on liposomes did not successfully disassemble soluble SNARE complexes. It can thus be concluded that, like α-SNAP, Sec17 efficacy is higher when the target complexes are incorporated into membranes. Similarly, the higher efficiency of SNAPs on membranes was not restricted to disassembly of the neuronal SNARE complex target, but was also observed for the disassembly of membrane-inserted yeast SNARE complexes (data not shown).

Complexin 1 Interferes with Disassembly of SNARE Complexes—The SNARE complex-interacting protein complexin has been reported to displace α-SNAP from SNARE complexes (46), thereby inhibiting the disassembly reaction. Meanwhile its crystal structure when bound to the SNARE complex has been solved (47, 48), revealing that complexin binds to a groove of the four-helix bundle formed by the helices of syntaxin 1a and synaptobrevin 2. In fact, it is easy to envision that bound complexin can interfere with the activity of the disassembly machinery, especially considering that complexin binds with very high affinity (49). Gel-based experiments, however, did not corroborate the inhibitory role of complexin (49). As such experiments only have a limited resolution and are mainly suited to detect strong effects, we re-investigated the influence

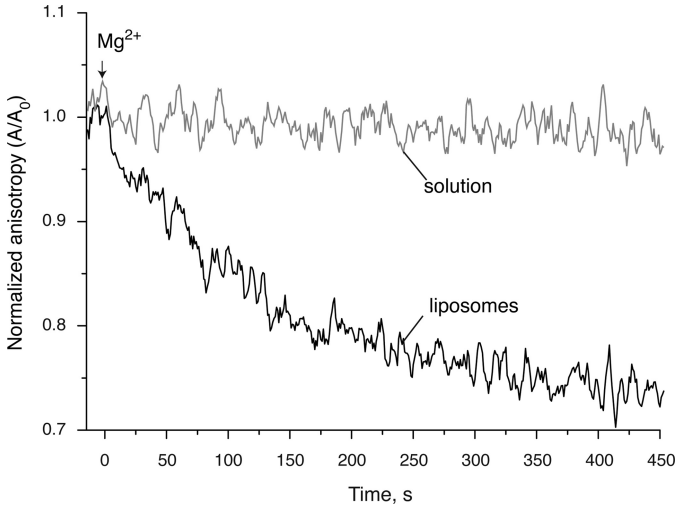

FIGURE 6. **The yeast SNAP homolog Sec17 shows membrane dependence as well.** Roughly 700 nM Sec17 and 1.5 nM NSF were able to disassemble 40 nM of membrane-inserted SNARE complexes (SybTMR^{C28TR}:SNAP25:SyxH3). The same amount of Sec17 did not promote disassembly of 40 nM SNARE complex in solution (Syb^{C28TR}:SNAP25:SyxH3). The reactions were started by the addition of 5 mM $MgCl_2$ (*arrow*). Note that even though the non-cognate combination of yeast Sec17 and mammalian NSF disassemble neuronal SNARE complexes less efficiently than the combination of Sec17 and Sec18, we chose to perform this experiment with this combination, because Sec18 was very fragile and tended to lose its activity rapidly.

of complexin on SNARE disassembly *in vitro* using our fluorescence-based assays. To this end, disassembly was carried out as usual except that complexin was added to the solution prior to the reaction trigger. We found that, in solution, 370 nM Cpx1 were able to inhibit SNARE disassembly strongly at an α-SNAP concentration of 1.1 μM, confirming that complexin is indeed able to interfere with the disassembly process (Fig. 7*a*). When disassembling liposomal complexes, the same amount of Cpx1 (370 nM) was needed to inhibit disassembly to a comparable extent, even though far less α-SNAP (45 nM) was present. This inhibition was completely overcome when 450 nM α-SNAP

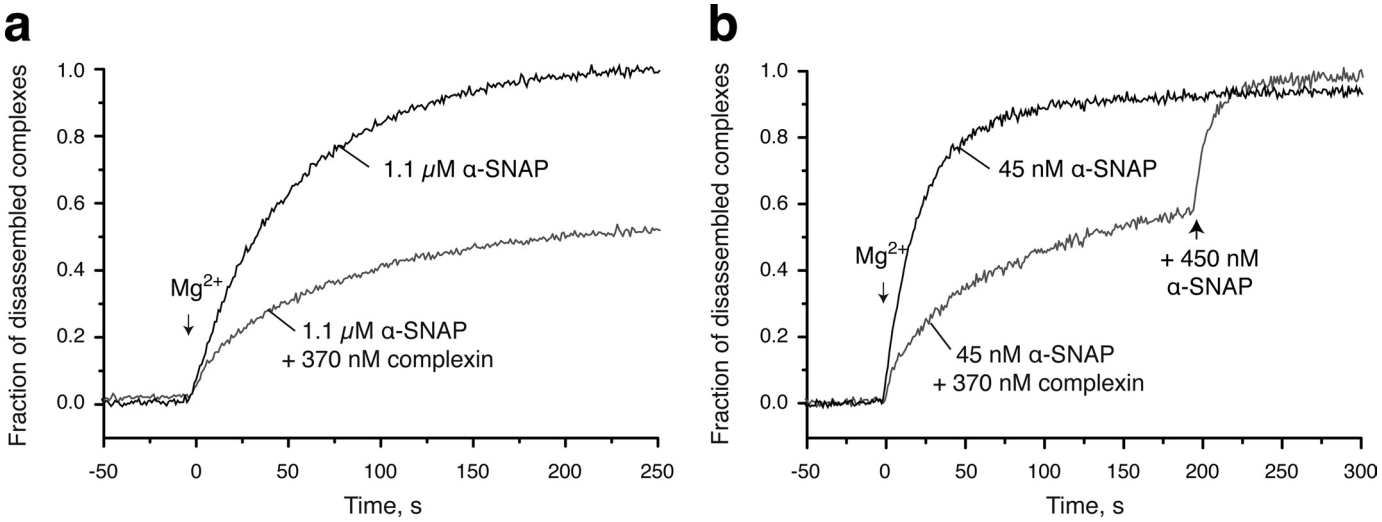

FIGURE 7. **The SNARE complex-interacting protein complexin 1 interferes more efficiently with disassembly in solution than on membranes.** *a*, in solution, substoichiometric amounts of Cpx 1 reduced α-SNAP efficiency during disassembly. Soluble, FRET-active complexes (Syb^{C28TR}:SNAP25^{C130TR}:SyxH3, ~75 nM) were disassembled by 4.5 nM NSF with the help of 1.1 μM α-SNAP in the presence or absence of 370 nM Cpx1. *b*, for the disassembly of membrane-inserted SNARE complexes, ~20 times less α-SNAP was needed. Accordingly, 45 nM α-SNAP was added to disassemble ~75 nM liposomal SNARE complex (SybTMR^{C28TR}:SNAP25^{C130TR}:SyxH3). Addition of 370 nM Cpx 1 inhibited the reaction on membranes as well, but the inhibition could be overcome effortlessly when an additional 450 nM α-SNAP was added (indicated by an *arrow*). Note that in this reaction, less than half the amount of α-SNAP is present compared with the reaction shown in *panel a*. This corroborates the view that affinity of α-SNAP to the SNARE bundle is augmented in the presence of the membrane.

were added (Fig. 7*b*). If one assumes that the affinity of Cpx1 does not vary drastically between liposomal and soluble complexes, this finding corroborates that α-SNAP binds with higher affinity to membrane-bound SNARE complexes.

DISCUSSION

The key function of the ATPase NSF is the disassembly of tight cis-SNARE complexes that arise form the fusion of a transport vesicle with its target membrane. NSF does not bind directly to the SNARE complex, but requires the adaptor α-SNAP. According to the current model, three copies of α-SNAP bind to the rod-like SNARE complex along its length (14). Although the approximate architecture of the entire 20S particle has been established for about a decade (19, 50), progress in understanding the disassembly mechanism, *i.e.* how NSF and α-SNAP take apart the tight SNARE bundle, has been surprisingly slow. Furthermore, it has remained unclear how much of the cofactor α-SNAP is required for NSF-driven SNARE complex disassembly. It seemed that nM amounts of α-SNAP were sufficient to saturate SNARE complex binding in some studies, whereas others reported an EC_{50} as high as 5 μM α-SNAP. As the studies used different methods, no clear parameter causing such differences was identifiable between the various studies.

One reason for these conflicting results might be because the disassembly factors are biochemically rather difficult to handle and so building up a reliable enzymatic assay with high-time resolution is challenging. A major step toward such an assay has been achieved recently by using a FRET assay based on GFP-variants of the SNARE proteins. Here, we have taken this approach a step forward by specifically labeling the SNARE proteins with fluorescent dyes. This approach avoided the bulky GFP moiety, allowing us to use a variety of different SNARE constructs, even the ones containing their transmembrane domains. In turn, the high time-resolution and flexibility of our assay allowed us to establish a protocol for a consistent preparation of highly active disassembly enzymes. We noticed that some of the proteins we used were more difficult to maintain in an active state. For example, due to ongoing degradation of β-SNAP during purification, the efficiencies of α-SNAP and β-SNAP could not be compared in an absolute manner. A degradation product of β-SNAP appears to be capable of inhibiting the disassembly reaction, which might explain why this homologue has been claimed to have a different role from α-SNAP in earlier studies (51, 52), although the proteins show 83% sequence identity (53). Despite the stability problem, and in agreement with another study (54), we were able to show that both proteins behave in a very similar manner during disassembly.

It soon became evident that when we used the soluble SNARE complex, the α-SNAP requirements agree with those studies reporting a low α-SNAP affinity: μM amounts of α-SNAP were needed to achieve optimal disassembly and to saturate SNARE complex binding. However, when we incorporated the SNARE complex into liposome membranes, much lower α-SNAP concentrations (~100 nM at most) were sufficient. This is comparable to the α-SNAP concentration recently found to disassemble SNARE complexes efficiently in "*ex vivo*" membrane sheets. Our results strongly suggest that α-SNAP is capable of interacting directly with membrane lipids, increasing its efficiency.

It is conceivable that the additional membrane attachment site serves to stabilize the interaction between α-SNAP and the SNARE rod, thereby substantially improving the efficiency of the disassembly process. We found similar activity increases for the α-SNAP homologs β-SNAP and Sec17, suggesting that SNAP cofactors in general are able to interact with the membrane. It had been proposed early on that SNAP cofactors might primarily recognize the overall shape of the four-helix bundle of

the SNARE complex, because the disassembly enzymes must be able to attack all the different types of SNARE complexes within the cell. Our results show that the affinity of SNAP to the core four-helix bundle, be it the neuronal SNARE complex or the yeast secretory complex, is only moderate. This suggests that the additional membrane attachment site is necessary to improve the overall affinity. The membrane might also function as a SNAP collector, providing a first SNAP binding site and thereby increasing its local concentration on the membrane, facilitating binding to cis-SNARE complexes. Alternatively, the membrane interaction might induce a conformational change in SNAP that strengthens its binding to the SNARE complex.

In our assay, complexin was able to inhibit disassembly of cis-SNARE complexes. The fact that this inhibition can be overcome by an increase in the α-SNAP concentration suggests that both proteins compete for binding to the SNARE complex. Because of the increased efficiency of α-SNAP on membranes, much less α-SNAP was needed to overcome complexin inhibition on liposomes than in solution. From this, we conclude that the affinity of complexin to the SNARE bundle is not increased by the presence of membranes in the same way as the affinity of α-SNAP. This is in line with the literature, where the affinity of complexin to the SNARE bundle has been reported to be even lower on membranes (55) than in solution (49). One could imagine that this helps to secure binding of SNAPs and complexin at the relevant stage of the SNARE cycle: SNAREs in cis-configuration might offer a high affinity binding site for SNAPs, whereas complexin might favor SNAREs in trans-configuration.

Our results demonstrate that NSF-catalyzed disassembly of SNARE complexes needs to be studied in the context of the lipid bilayer. Only when the high affinity SNAP binding site is established can stoichiometric amounts of α-SNAP be used. This is important, because unnaturally high α-SNAP requirements may occlude bottlenecks of the reaction or regulatory mechanisms. Certainly, this should also help to decode the protein-protein interactions during disassembly. For example, even though three α-SNAPs may bind to one SNARE complex in purified 20S complexes, as determined by quantitative amino acid analysis (14), it is not known whether three α-SNAPs actually have to be bound for functional disassembly.

Based on a multitude of mutations on the surface of α-SNAP, an α-SNAP:SNARE complex binding model has been generated. This model is based on shape and charge complementary between the surface of α-SNAP and the SNARE complex (20). In this model, the N-terminal region of α-SNAP points outwards. Remarkably, the C-terminal globular bundle domain of α-SNAP had to be taken out of the model in order to avoid a clash between the α-SNAP and the SNARE complex. Therefore, the authors suggested that the C-terminal domain of α-SNAP might bend upon binding to the SNARE complex (20). Of course, such a scenario cannot be ruled out by our findings. Yet if one assumes, that the conformation of α-SNAP does not change drastically upon binding, binding of α-SNAP alongside the SNARE bundle would position the N-terminal region of α-SNAP more toward the lipid bilayer (Fig. 4*a*). The N-terminal region consists of a twisted sheet of nine α-helices. The first two helices are connected by an extended loop that sticks out of the twisted sheet. The loop contains mostly hydrophobic amino acids (residues 27–32), suggesting that it accommodates the membrane attachment site. Indeed, the presence of the membrane did not longer improve the disassembly reaction when we deleted the entire putative membrane anchor region (aa 1–32) or, more subtly, when the two highly conserved phenylalanine residues (F27S, F28S) on the extended loop in α-SNAP were mutated. These phenylalanines appear to be perfectly suited to sink into the lipid bilayer, where they can anchor the protein. It should be noted that the mutant efficiency in solution was comparable to that of wild-type α-SNAP, indicating that despite their fundamental importance for lipid binding, the two phenylalanine residues are not involved in SNAP-SNARE or SNAP-NSF interaction. Interestingly, the homologous loop is shorter in γ-SNAP, a distantly related isoform, and adopts a different local conformation (43). Nevertheless, the loop in γ-SNAP also contains exposed aromatic residues, Phe-23 and Trp-26, which might be able to interact with a membrane. Taken together, these findings strongly suggest that the hook-like structure is essential for a protein-lipid interaction that potentiates the α-SNAP efficiency during SNARE complex disassembly. Hence, the disassembly machinery seems perfectly adapted to attack membrane-inserted SNARE bundles.

Acknowledgments—We thank Alexander Stein, Ursel Ries, and Wolfgang Berning-Koch for protein preparations and Thorsten Lang and Dana Bar-On for fruitful discussions.

REFERENCES

1. Jahn, R., and Scheller, R. H. (2006) *Nat. Rev.* **7,** 631–643
2. Rizo, J., and Rosenmund, C. (2008) *Nat. Struct. Mol. Biol.* **15,** 665–674
3. Martens, S., and McMahon, H. T. (2008) *Nat. Rev.* **9,** 543–556
4. Südhof, T. C., and Rothman, J. E. (2009) *Science* **323,** 474–477
5. Hayashi, T., McMahon, H., Yamasaki, S., Binz, T., Hata, Y., Südhof, T. C., and Niemann, H. (1994) *EMBO J.* **13,** 5051–5061
6. Fasshauer, D., Antonin, W., Subramaniam, V., and Jahn, R. (2002) *Nat. Struct. Biol.* **9,** 144–151
7. Wiederhold, K., and Fasshauer, D. (2009) *J. Biol. Chem.,* **284,** 13143–13152
8. Malhotra, V., Orci, L., Glick, B. S., Block, M. R., and Rothman, J. E. (1988) *Cell* **54,** 221–227
9. Hanson, P. I., Roth, R., Morisaki, H., Jahn, R., and Heuser, J. E. (1997) *Cell* **90,** 523–535
10. Fleming, K. G., Hohl, T. M., Yu, R. C., Müller, S. A., Wolpensinger, B., Engel, A., Engelhardt, H., Brünger, A. T., Söllner, T. H., and Hanson, P. I. (1998) *J. Biol. Chem.* **273,** 15675–15681
11. Furst, J., Sutton, R. B., Chen, J., Brunger, A. T., and Grigorieff, N. (2003) *EMBO J.* **22,** 4365–4374
12. Hohl, T. M., Parlati, F., Wimmer, C., Rothman, J. E., Söllner, T. H., and Engelhardt, H. (1998) *Mol. Cell* **2,** 539–548
13. Clary, D. O., Griff, I. C., and Rothman, J. E. (1990) *Cell* **61,** 709–721
14. Wimmer, C., Hohl, T. M., Hughes, C. A., Müller, S. A., Söllner, T. H., Engel, A., and Rothman, J. E. (2001) *J. Biol. Chem.* **276,** 29091–29097
15. Söllner, T., Bennett, M. K., Whiteheart, S. W., Scheller, R. H., and Rothman, J. E. (1993) *Cell* **75,** 409–418
16. Söllner, T., Whiteheart, S. W., Brunner, M., Erdjument-Bromage, H., Geromanos, S., Tempst, P., and Rothman, J. E. (1993) *Nature* **362,** 318–324
17. Brunger, A. T., and DeLaBarre, B. (2003) *FEBS Lett.* **555,** 126–133
18. Brunger, A. T. (2005) *Q. Rev. Biophys.* **38,** 1–47
19. Zhao, C., Slevin, J. T., and Whiteheart, S. W. (2007) *FEBS Lett.* **581,** 2140–2149

20. Marz, K. E., Lauer, J. M., and Hanson, P. I. (2003) *J. Biol. Chem.* **278,** 27000–27008
21. Lauer, J. M., Dalal, S., Marz, K. E., Nonet, M. L., and Hanson, P. I. (2006) *J. Biol. Chem.* **281,** 14823–14832
22. Hibi, T., Hirashima, N., and Nakanishi, M. (2000) *Biochem. Biophys. Res. Commun.* **271,** 36–41
23. Hirling, H., and Scheller, R. H. (1996) *Proc. Natl. Acad. Sci. U.S.A.* **93,** 11945–11949
24. Morgan, A., and Burgoyne, R. D. (1995) *EMBO J.* **14,** 232–239
25. Hayashi, T., Yamasaki, S., Nauenburg, S., Binz, T., and Niemann, H. (1995) *EMBO J.* **14,** 2317–2325
26. Bar-On, D., Winter, U., Nachliel, E., Gutman, M., Fasshauer, D., Lang, T., and Ashery, U. (2008) *FEBS Lett.* **582,** 3563–3568
27. Ungermann, C., Sato, K., and Wickner, W. (1998) *Nature* **396,** 543–548
28. Fasshauer, D., Eliason, W. K., Brünger, A. T., and Jahn, R. (1998) *Biochemistry* **37,** 10354–10362
29. Fasshauer, D., Antonin, W., Margittai, M., Pabst, S., and Jahn, R. (1999) *J. Biol. Chem.* **274,** 15440–15446
30. Fasshauer, D., and Margittai, M. (2004) *J. Biol. Chem.* **279,** 7613–7621
31. Pabst, S., Hazzard, J. W., Antonin, W., Südhof, T. C., Jahn, R., Rizo, J., and Fasshauer, D. (2000) *J. Biol. Chem.* **275,** 19808–19818
32. Margittai, M., Fasshauer, D., Pabst, S., Jahn, R., and Langen, R. (2001) *J. Biol. Chem.* **276,** 13169–13177
33. Margittai, M., Otto, H., and Jahn, R. (1999) *FEBS Lett.* **446,** 40–44
34. Barszczewski, M., Chua, J. J., Stein, A., Winter, U., Heintzmann, R., Zilly, F. E., Fasshauer, D., Lang, T., and Jahn, R. (2008) *Mol. Biol. Cell* **19,** 776–784
35. Barnard, R. J., Morgan, A., and Burgoyne, R. D. (1997) *J. Cell Biol.* **139,** 875–883
36. Stein, A., Radhakrishnan, A., Riedel, D., Fasshauer, D., and Jahn, R. (2007) *Nat. Struct. Mol. Biol.* **14,** 904–911
37. Nagy, A., Baker, R. R., Morris, S. J., and Whittaker, V. P. (1976) *Brain Res.* **109,** 285–309
38. Takamori, S., Holt, M., Stenius, K., Lemke, E. A., Grønborg, M., Riedel, D., Urlaub, H., Schenck, S., Brügger, B., Ringler, P., Müller, S. A., Rammner, B., Gräter, F., Hub, J. S., De Groot, B. L., Mieskes, G., Moriyama, Y., Klingauf, J., Grubmüller, H., Heuser, J., Wieland, F., and Jahn, R. (2006) *Cell* **127,** 831–846
39. Matveeva, E. A., He, P., and Whiteheart, S. W. (1997) *J. Biol. Chem.* **272,** 26413–26418
40. Whiteheart, S. W., Brunner, M., Wilson, D. W., Wiedmann, M., and Rothman, J. E. (1992) *J. Biol. Chem.* **267,** 12239–12243
41. Morgan, A., Dimaline, R., and Burgoyne, R. D. (1994) *J. Biol. Chem.* **269,** 29347–29350
42. Steel, G. J., Buchheim, G., Edwardson, J. M., and Woodman, P. G. (1997) *Biochem. J.* **325,** 511–518
43. Bitto, E., Bingman, C. A., Kondrashov, D. A., McCoy, J. G., Bannen, R. M., Wesenberg, G. E., and Phillips, G. N., Jr. (2008) *Proteins* **70,** 93–104
44. Rice, L. M., Brennwald, P., and Brünger, A. T. (1997) *FEBS Lett.* **415,** 49–55
45. Griff, I. C., Schekman, R., Rothman, J. E., and Kaiser, C. A. (1992) *J. Biol. Chem.* **267,** 12106–12115
46. McMahon, H. T., and Südhof, T. C. (1995) *J. Biol. Chem.* **270,** 2213–2217
47. Chen, X., Tomchick, D. R., Kovrigin, E., Arac, D., Machius, M., Südhof, T. C., and Rizo, J. (2002) *Neuron* **33,** 397–409
48. Bracher, A., Kadlec, J., Betz, H., and Weissenhorn, W. (2002) *J. Biol. Chem.* **277,** 26517–26523
49. Pabst, S., Margittai, M., Vainius, D., Langen, R., Jahn, R., and Fasshauer, D. (2002) *J. Biol. Chem.* **277,** 7838–7848
50. Hanson, P. I., and Whiteheart, S. W. (2005) *Nat. Rev.* **6,** 519–529
51. Schiavo, G., Gmachl, M. J., Stenbeck, G., Söllner, T. H., and Rothman, J. E. (1995) *Nature* **378,** 733–736
52. Xu, J., Xu, Y., Ellis-Davies, G. C., Augustine, G. J., and Tse, F. W. (2002) *J. Neurosci.* **22,** 53–61
53. Whiteheart, S. W., Griff, I. C., Brunner, M., Clary, D. O., Mayer, T., Buhrow, S. A., and Rothman, J. E. (1993) *Nature* **362,** 353–355
54. Sudlow, A. W., McFerran, B. W., Bodill, H., Barnard, R. J., Morgan, A., and Burgoyne, R. D. (1996) *FEBS Lett.* **393,** 185–188
55. Bowen, M. E., Weninger, K., Ernst, J., Chu, S., and Brunger, A. T. (2005) *Biophys. J.* **89,** 690–702
56. Rice, L. M., and Brunger, A. T. (1999) *Mol. Cell* **4,** 85–95
57. Stein, A., Weber, G., Wahl, M. C., and Jahn, R. (2009) *Nature* **460,** 525–528